Arabian Journal of Chemistry 16 (2023) 105279

Contents lists available at ScienceDirect

Arabian Journal of Chemistry

journal homepage: www.sciencedirect.com

Original article

Synthesis and biological evaluation of chromone-thiazolidine-2,4-dione derivatives as potential α-glucosidase inhibitors

Yingying Zheng [a], Mengyu Li [a], Simin Wu [a], Lu Li [a], Zhuang Xiong [a], Xuetao Xu [a,*], Kun Zhang [a,*], Yi Wen [b,*]

[a] Guangdong Provincial Key Laboratory of Large Animal Models for Biomedicine, School of Biotechnology and Health Sciences, Wuyi University, Jiangmen 529020, China
[b] Department of Pharmacy, Zhongshan City People's Hospital, Zhongshan 528403, China

ARTICLE INFO

Article history:
Received 26 March 2023
Accepted 16 September 2023
Available online 22 September 2023

Keywords:
Chromone
Thiazolidine-2,4-dione
α-Glucosidase
Inhibitor

ABSTRACT

A series of chromone-thiazolidine-2,4-dione derivatives (**e1** ~ **28**) were synthesized and screened for their α-glucosidase inhibitory. All synthetic derivatives presented excellent α-glucosidase inhibitory with IC_{50} values ranging from 2.40 ± 0.11 to 5.66 ± 0.15 μM, comparing to positive control acarbose (IC_{50} value: 640.57 ± 5.13 μM). Among them, compound **e28** displayed the strongest α-glucosidase inhibitory (IC_{50} value: 2.40 ± 0.11), ~267 times stronger than positive control acarbose. Kinetic studies revealed that compound **e28** was a reversible non-competitive inhibitor. CD spectra and 3D fluorescence spectra results explained that compound **e28** changed the conformational changes of α-glucosidase. Molecular docking simulated the binding between compound **e28** and α-glucosidase. *In vitro* cytotoxicity assay ascertained the good security of **e28**.

1. Introduction

Type 2 diabetes (T2D) is a common chronic metabolic disease characterized by hyperglycemia threatening human health worldwide (Heydari et al., 2010; Cho et al., 2018). Hyperglycemia is mainly caused by defective insulin secretion and long-term hyperglycemia leads to chronic damage and dysfunction of various tissues, especially eyes, kidneys, hearts, blood vessels and nerves (Pogaku et al., 2019; Bushra et al., 2021). α-Glucosidase has been confirmed as one important therapeutic target for T2D (Saxena et al., 2021; Hameed et al., 2019). As an important membrane bound enzyme located in small intestine, α-glucosidase catalyzes the hydrolysis of carbohydrates, resulting in release of absorbable single glucose (Dhameja and Gupta, 2019; Zhu et al., 2020). Inhibiting the α-glucosidase activity can delay the hydrolysis and absorption of carbohydrates, lowering the postprandial blood glucose (Coleman et al., 2019; Zhang et al., 2019). Although several α-glucosidase inhibitors have been used as clinical drugs to treat T2D, such as acarbose, voglibose, and miglitol, but they still have some gastrointestinal side effects. Therefore, discovery of potential α-glucosidase inhibitors is essential for the development of hypoglycemic drugs.

Chromone, one important oxygen containing heterocyclic compound, widely exists in natural products (Demetgül and Beyazit, 2018). Chromone has been confirmed as a privileged scaffold to develop novel bioactive molecules due to its multiple pharmacological activities, including antioxidant, anti-inflammatory, anticancer, and antibacterial activities (Lai et al., 2021; Prakash et al., 2008; Liu et al., 2020; Shatokhin et al., 2022). Moreover, some chromone derivatives have been reported to present α-glucosidase inhibitory activity (Fig. 1) (Fan et al., 2023; Fan et al., 2023; Wang et al., 2018). On the other hand, thiazolidine-2,4-dione (TZD) is an important moiety exhibiting broad range of biological activities, such as antidiabetic activity, anti-inflammatory and anticancer (Diamant and Heine, 2003; Chaudhry et al., 2007; Shaikh et al., 2015). Its derivatives rosiglitazone and pioglitazone have been used as clinical drugs for T2D. Recently, some TZD derivatives have been developed as α-glucosidase inhibitors (Thari et al., 2022; Fettach et al., 2023; Hussain et al., 2019) (Fig. 1).

Pharmacophore hybridization is a useful strategy in new drug development, that hybridizes two or more pharmacophore to create a new compound with more efficacy and affinity. In view of α-glucosidase inhibitory activities of chromone and TZD and in continuation of our interest in the development of potential α-glucosidase inhibitors, it was envisaged to hybridize chromone

* Corresponding authors.
E-mail addresses: wyuchemxxt@126.com (X. Xu), zssrmyywenyi@163.com (Y. Wen).

Peer review under responsibility of King Saud University.

Production and hosting by Elsevier

https://doi.org/10.1016/j.arabjc.2023.105279
1878-5352/

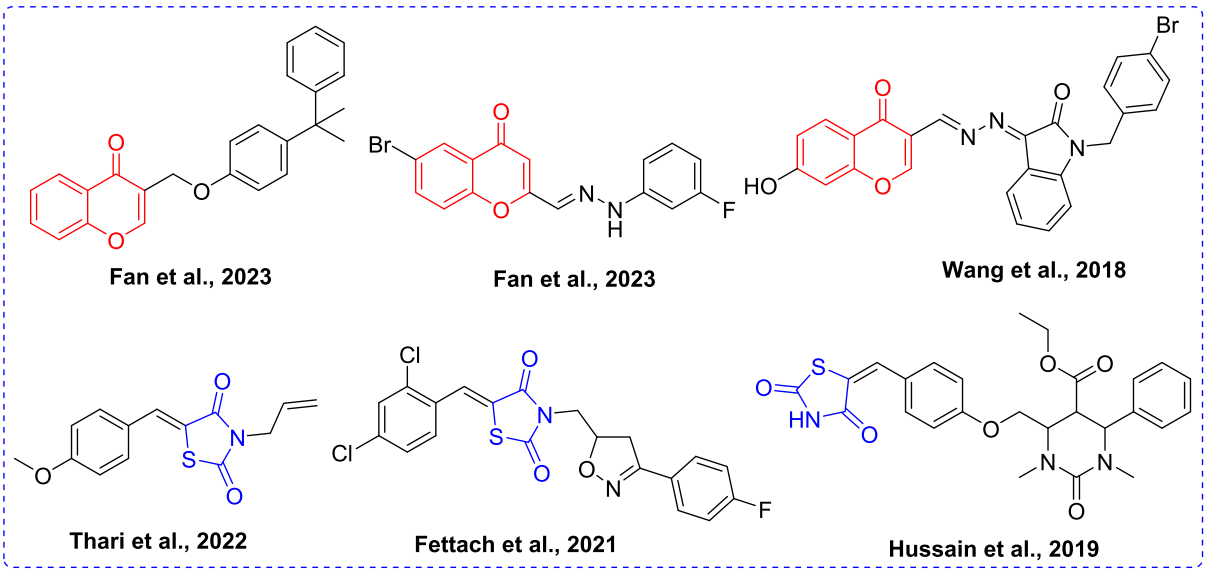

Fig. 1. Some α-glucosidase inhibitors containing chromone or TZD.

and TZD pharmacophores in one molecular skeleton to yield potential lead compound toward α-glucosidase. Herein, we synthesize a series chromone-TZD derivatives and evaluated their α-glucosidase inhibitory activities and mechanism.

2. Results and discussion

2.1. Chemistry

Chromone-TZD derivatives (**e1** ∼ **28**) were synthesized according to listed Schemes 1**.** TZD (**a**) underwent substitution reaction with ethyl bromoacetate to produce intermediate **b**, which reacted with chromene-3-carbaldehyde to obtain intermediate **c**. Compound **c** was hydrolyzed to yield intermediate **d**, which underwent condensation reaction with anilines to get the target derivatives (**e1** ∼ **28**). All compounds had been characterized and confirmed by ^{1}H NMR, ^{13}C NMR and HRMS.

2.2. α-Glucosidase inhibition evaluation and SAR analysis

The α-glucosidase inhibitory of chromone-TZD derivatives (**e1** ∼ **28**) was detected using α-glucosidase from *Saccharomyces cerevisiae* and the inhibition results were summarized in Table 1. All synthetic derivatives presented excellent α-glucosidase inhibitory with IC_{50} values ranging from 2.40 ± 0.11 to 5.66 ± 0.15 μM, which were obviously lower than that of positive control acarbose (IC_{50} value: 640.57 ± 5.13 μM). Among them, compound **e28** displayed the strongest α-glucosidase inhibitory (IC_{50} value: 2.40 ± 0.11), ∼ 267 times stronger than positive control acarbose.

2.3. Inhibitory kinetic studies

Compound **e28** with the strongest α-glucosidase inhibitory was selected as representative compound to analyze the inhibition mechanism on α-glucosidase. For enzyme kinetics, the absorbance change of test system with different concentration of α-glucosidase and compound **e28** was detected. The resulting plots of compound **e28** with different concentration all passed the origin (Fig. 2A) with different slope, suggesting a reversible inhibitor. For substrate kinetics, the absorbance change of test system with different concentration of substrate and compound **e28** was detected. The obtaining Lineweaver-Burk plots of compound **e28** with different concentration intersected at one point of *x*-axis (Fig. 2B), indicating a non-competitive inhibition mode.

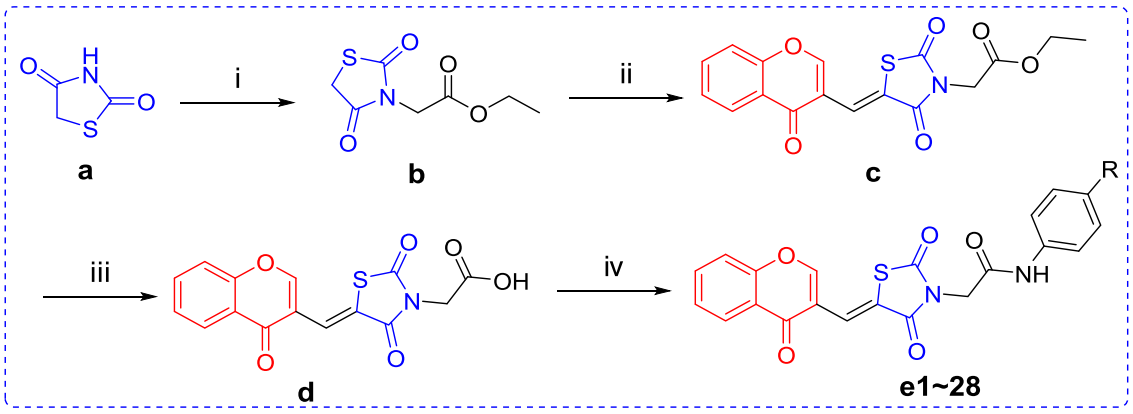

Scheme 1. Reaction conditions and reagents: (i) Ethyl Bromoacetate, K_2CO_3, Acetone, Reflux; (ii) Chromene-3-carbaldehyde, AcONa, AcOH, Reflux; (iii) 12 N HCl, AcOH, Reflux; (iv) Anilines, EDCI, Pyridine, rt.

Table 1
α-Glucosidase inhibition of chromone-TZD derivatives (**e1** ∼ **28**).

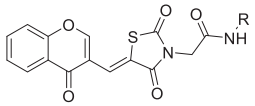

Inhibitor	R	IC_{50} (μM)	Inhibitor	R	IC_{50} (μM)
e1		5.66 ± 0.15	**e15**		5.37 ± 0.18
e2		4.34 ± 0.26	**e16**		4.26 ± 0.16
e3		3.83 ± 0.15	**e17**		4.68 ± 0.14
e4		5.32 ± 0.24	**e18**		5.62 ± 0.22
e5		3.93 ± 0.15	**e19**		3.74 ± 0.12
e6		3.45 ± 0.13	**e20**		5.24 ± 0.21
e7		4.57 ± 0.16	**e21**		5.42 ± 0.15
e8		3.84 ± 0.12	**e22**		4.89 ± 0.18
e9		2.79 ± 0.11	**e23**		4.19 ± 0.14
e10		4.98 ± 0.16	**e24**	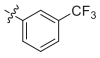	5.20 ± 0.15
e11		4.71 ± 0.12	**e25**	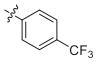	4.98 ± 0.14
e12	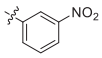	3.65 ± 0.10	**e26**		3.12 ± 0.13
e13	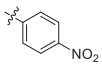	5.18 ± 0.12	**e27**		2.95 ± 0.23
e14		4.33 ± 0.27	**e28**		2.40 ± 0.11
Acarbose		640.57 ± 5.13			

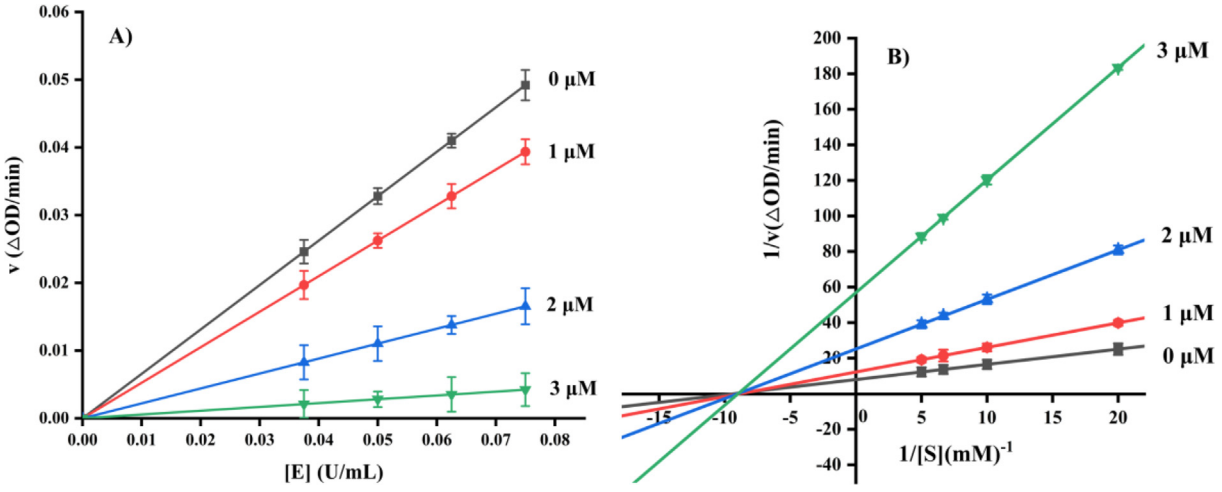

Fig. 2. Inhibitory kinetic studies of compound **e28**.

2.4. CD spectra

Circular dichroism (CD) spectra was conducted to analyze the effect of compound **e28** on the conformational changes of α-glucosidase. As shown in Fig. 3, CD spectra of α-glucosidase appeared two characteristic peaks at 210 and 222 nm, which could reflect the change of α-helix peptide bond. It was also seen that compound **e28** treatment changed the peak size and shape of α-glucosidase, revealing that compound **e28** caused the conformational changes of α-glucosidase. The conformational changes of α-glucosidase by compound **e28** were calculated and listed in Table 2. Compound **e28** treatment (molar ratios: 3:1) caused the increase of α-helix (from 10.4 to 11.3%), β-sheet (from 31.2 to 31.7%), and β-turn (from 20.1 to 20.2%), respectively, while the decrease of random coil (from 33.2 to 32.5%).

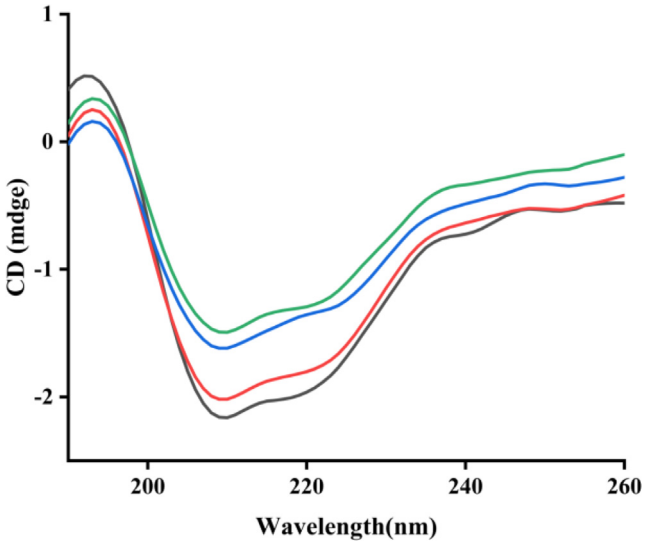

Fig. 3. CD spectra of α-glucosidase with compound **e28**. Molar ratios of α-glucosidase to compound **e28**: 1:0 (Black line), 1:1 (Red line), 1:2 (Blue line), 1:3 (Green line).

Table 2
The secondary structural changes of α-glucosidase.

Molar ratio [enzyme]: [**e28**]	α-Helix (%)	β-Sheet (%)	β-turn (%)	Random coil (%)
1:0	10.4	31.2	20.1	33.2
1:1	10.4	31.2	20.1	33.2
1:2	11.2	32.3	20.0	32.3
1:3	11.3	31.7	20.2	32.5

2.5. 3D fluorescence spectra

Three-dimensional (3D) fluorescence spectra was monitored to conformational changes of α-glucosidase. Fig. 4A was the 3D fluorescence spectra of α-glucosidase, presenting two characteristic peaks corresponding to tyrosine and tryptophan residues (Peak **1**, $\lambda_{ex}/\lambda_{em}$: 276/330 nm) and peptide backbone structure (Peak **2**, $\lambda_{ex}/\lambda_{em}$: 232/332 nm). While compound **e28** treatment (2 μM) lead to the fluorescence intensity reduction of Peak **1** by 30.0% and Peak **2** by 61.5% (Fig. 4B). The results suggested that the binding between compound **e28** and α-glucosidase could cause the conformational change of enzyme.

2.6. Docking analysis

Molecular docking was used to simulate the binding between compound **e28** and α-glucosidase. The docking results (Fig. 5A-C) confirmed that compound **e28** bounded in the active pocket of α-glucosidase with a "V-shaped" configuration. Detailed binding analysis results (Fig. 5D) showed that one carbonyl of TZD formed one hydrogen bond with Asn241 (2.1 Å), the carbonyl of amide formed one hydrogen bond with Arg312 (2.5 Å), the oxygen of chromone formed one hydrogen bond with Arg312 (2.5 Å), one bromine formed one halogen bond with Gly159 (3.1 Å), and another bromine formed one halogen bond with Asn412 (3.4 Å). Moreover, compound **e28** formed hydrophobic interactions with Lys155, Ala278, Phe300, and Tyr313. Above hydrogen bond, halogen bond, and hydrophobic interaction helped compound **e28** to adopt in the active pocket of α-glucosidase.

2.7. In vitro cytotoxicity

The safety profile of compound **e28** was assayed by its *in vitro* cytotoxicity against human normal hepatocytes L-02 cells and human normal intestinal epithelial NCM460 cells using ATP assay. Due to the solubility of **e28**, we assayed its cells cytotoxicity up to maximum concentration of 100 μM. As shown in Fig. 6, compound **e28** treatment (0 ~ 100 μM) had no obvious effect on the viability of L-02 cells. Although **e28** (100 μM) treatment could reduce the cell viability of NCM460, but its IC_{50} value was higher than100 μM. These results suggested the good security of compound **e28** on L-02 cells and NCM460 cells at a low concentration.

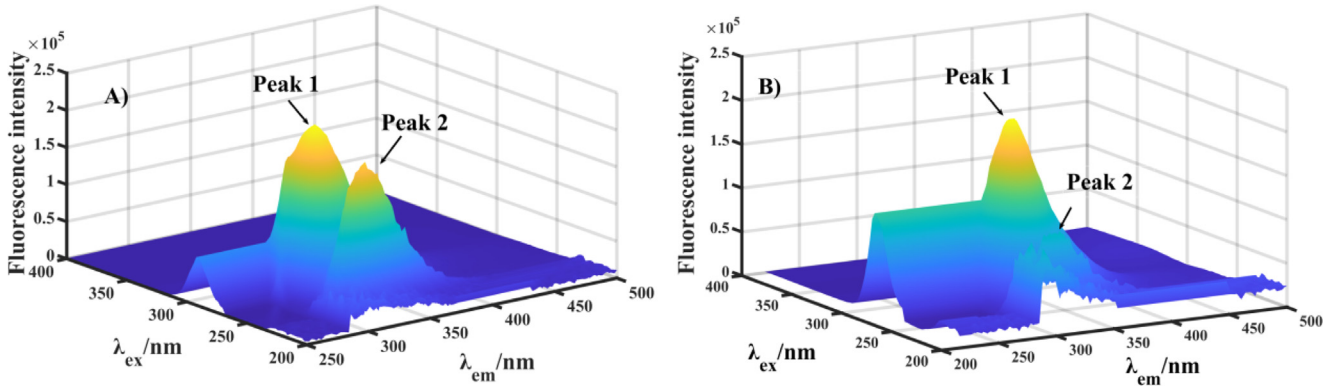

Fig. 4. The 3D fluorescence spectra of α-glucosidase with compound **e28**.

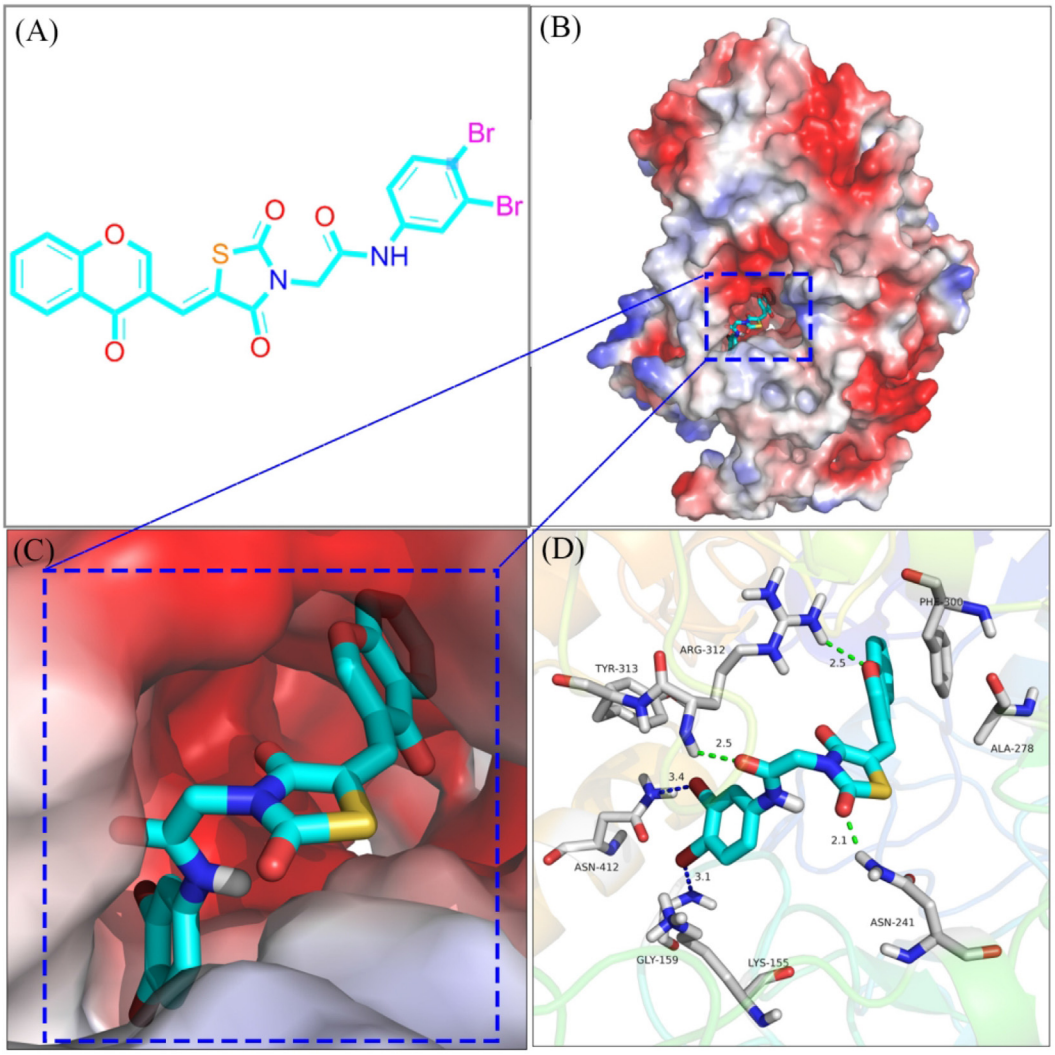

Fig. 5. The molecular docking α-glucosidase with compound **e28**.

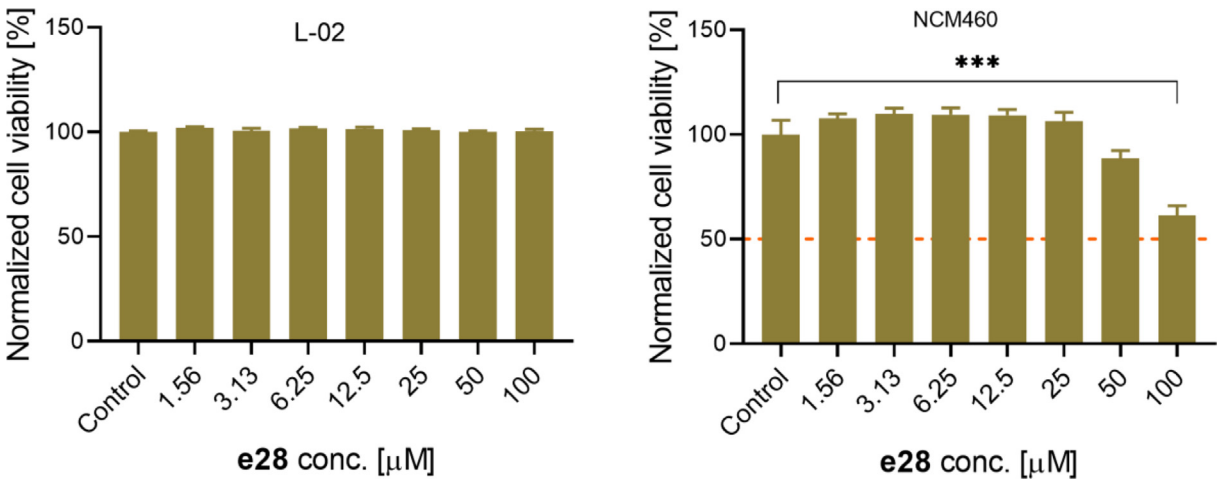

Fig. 6. *In vitro* cytotoxicity of compound **e28** against L-02 and NCM460 cells. Compared to control group, $^{***}P < 0.001$.

3. Conclusion

In summary, a series of Chromone-TZD derivatives (**e1** ∼ **28**) were synthesized as potential α-glucosidase inhibitors. Among them, compound **e28** with bis-bromine substituents on the benzene ring had the strongest α-glucosidase inhibitory activity with IC_{50} value of 2.40 ± 0.11 μM. SAR analysis showed that introduction of substituents on the benzene ring would contribute to α-

glucosidase inhibitory activity. Kinetic studies revealed that compound **e28** was a reversible non-competitive inhibitor. CD spectra and 3D fluorescence spectra results explained that compound **e28** changed the conformational changes of α-glucosidase. Molecular docking simulated the binding between compound **e28** and α-glucosidase. Moreover, *in vitro* cytotoxicity assay ascertained the good security of **e28**. Our study highlighted chromone-TZD derivatives as promising α-glucosidase inhibitors.

4. Experimental

*4.1. Synthesis of chromone-TZD derivatives (**e1** ∼ **28**)*

TZD (**a**) (3 mmol), ethyl bromoacetate (3 mmol), and K_2CO_3 (6 mmol) were added into acetone solution (3 mL) and refluxed reaction for 4 h. After reaction solution was filtered, the obtained solvent was removed to yield intermediate **b**. To the solution of **b** (2 mmol) in 2 mL glacial acetic acid, sodium acetate (2 mmol) and chromone-3-carboxaldehyde (2 mmol) were added and reacted for 5 h at 100 °C. After reaction solution was filtered, the obtained solid was washed with ethyl acetate to produce intermediate **c**. Compound **c** was added into 12 N HCl (2 mL) and glacial acetic acid (8 mL) to hydrolysis overnight at 100 °C. The solid was filtrated and washed to yield intermediate **d**. To the solution of **d** (2 mmol) in pyridine solution (2.5 mL), substituted anilines (2.2 mmol) and EDCI (2 mmol) were added and reacted overnight at room temperature. The solid was recrystallized using DMF to produce chromone-TZD derivatives (**e1** ∼ **28**). All NMR and HRMS data were shown in supplementary material.

4.2. a-Glucosidase inhibition and kinetics study

The α-glucosidase inhibitory activity of all compounds was screened according to our previous methods (Wang et al., 2017; Özil et al., 2017; Mermer et al., 2018). To 140 μL of α-glucosidase solution, test samples (10 μL) was added and incubated for 10 min at 37 °C, followed by the addition of *p*-NPG (50 μL). Then the absorbance change at 405 nm was measured. In the test system, the final concentrations of α-glucosidase and *p*-NPG were 0.1 U/mL and 0.25 mM, respectively. The inhibition rate of each sample was calculated based on the blank sample.

For enzyme kinetics, the α-glucosidase concentrations (0.075, 0.1, 0.125 and 0.15 U/mL) were used in test system and the absorbance change of compound **e28** with different concentration was measured (Huang et al., 2021; Khan et al., 2022; Ye et al., 2019). For substrate kinetics, the substrate concentrations (1.0, 2.0, 3.0, 4.0 mM) were used in test system and the absorbance change of compound **e28** with different concentration was measured. Lineweaver-Burk plots were used to analyze substrate kinetics (Zhang et al., 2022; Xu et al., 2020; Deng et al., 2022).

4.3. CD spectra

To 190 μL of α-glucosidase solution (31 μM), 10 μL of compound **e28** (31, 62, 124 μM) was added and incubated for 5 min. Then CD spectra were scanned from 190 to 260 nm. Also, the secondary structural parameters were calculated using CDNN software (Hu et al., 2021; Lin et al., 2023; Fan et al., 2023).

4.4. 3D fluorescence spectra

To 3.0 mL of α-glucosidase solution (5 μM), 10 μL of compound **e28** (2 μM) was added and incubated for 5 min. Then 3D fluorescence spectra were scanned with slit width of 2.5 nm at excitation and emission wavelengths from 200 to 600 nm (Wu et al., 2023; Lu et al., 2023; Li et al., 2023).

4.5. Molecular docking.

Molecular docking was conducted using SYBYL software according to previous methods (Wang et al., 2023; Peng et al., 2021; Xiao et al., 2023; Li et al., 2023). The homology model of α-glucosidase had been early build in our previous works. The α-glucosidase was optimized using the internal program and generated the active pocket. After the compound **e28** was prepared with charged and energy minimization, its docking with α-glucosidase was conducted in the default format.

4.5. ATP assay

We tested the cell viability by using CellTiter-Glo® Luminescent Cell Viability Assay (ATP assay). Human normal live cells L-02 cells (ATCC, EK-Bioscience) were cultured in RPMI-1640 with 10% fetal bovine serum and 1% penicillin and streptomycin. Human normal colon mucosal epithelial cell line NCM460 (FuHeng biology) were cultured in the DMEM with 10% fetal bovine serum and 1% penicillin and streptomycin.

L-02 cells and NCM460 cells were seeded on 96-well microplate for 24 h at a density of 1×10^4 cells / well and 0.5×10^4 cells / well, respectively. L-02 cells were treaed with different doses of **e28** (0, 1.56, 3.13, 6.25, 12.5, 25, 50, 100 μM) for 24 h. CellTiter-Glo Reagent was added to each well and shake the mix for 2 mins. Then the luminescent signal were read by an microplate reader (Perkin Elmer, EnVision® multilabel reader). Values are expressed as percentage of control. Statistical analysis was performed using GraphPad Prism 7.0. Data were expressed as Mean ± SD (n = 3); and P values were determined by one-way ANOVA; $^{*}P < 0.05$, $^{**}P < 0.01$, $^{***}P < 0.001$.

Declaration of Competing Interest

The authors declare that they have no known competing financial interests or personal relationships that could have appeared to influence the work reported in this paper.

Acknowledgements

This work was financially supported by the Department of Education of Guangdong Province (2021KCXTD044), Fundamental and Applied Basic Research Fund of Guangdong Province (2022A1515011657), the Science and Technology Planning Project of Guangdong Province (2021B1212040016), and Jiangmen Science and Technology Plan Project (202103010315000664, 2220002000375).

Appendix A. Supplementary data

Supplementary data to this article can be found online at https://doi.org/10.1016/j.arabjc.2023.105279.

References

Bushra, S., Shamim, K.M., Khan, N., Ullah, M., Mahdavi, M.A., Faramarzi, B., Larijani, U., Salar, R., Rafique, M., Taha, S., 2021. Perveen, synthesis, in vitro, and in silico evaluation of Indazole Schiff bases as potential α-glucosidase inhibitors. J. Mol. Struct. 1242, 130826.

Chaudhry, J., Ghosh, N.N., Roy, K., Chandra, R., 2007. Antihyperglycemic effect of a new thiazolidinedione analogue and its role in ameliorating oxidative stress in al- loxan-induced diabetic rats. Life Sci. 80, 1135–1142.

Cho, N.H., Shaw, J.E., Karuranga, S., Huang, Y., da Rocha Fernandes, J.D., Ohlrogge, A. W., Malanda, B., 2018. IDF Diabetes Atlas: global estimates of diabetes prevalence for 2017 and projections for 2045, Diabetes Res. Clin. Pract. 138, 271–281.

Coleman, R.L., Scott, C.A.B., Lang, Z., Bethel, M.A., Tuomilehto, J., Holman, R.R., 2019. Meta-analysis of the impact of alpha-glucosidase inhibitors on incident diabetes and cardiovascular outcomes. Cardiovasc. Diabetol. 18, 135.
Demetgül, C., Beyazit, N., 2018. Synthesis, characterization and antioxidant activity of chitosan-chromone derivatives. Carbohyd. Polym. 181, 812–817.
Deng, X.Y., Ke, J.J., Zheng, Y.Y., Li, D.L., Zhang, K., Zheng, X., Wu, J.Y., Xiong, Z., Wu, P. P., Xu, X.T., 2022. Synthesis and bioactivities evaluation of oleanolic acid oxime ester derivatives as α-glucosidase and α-amylase inhibitors. J. Enzyme, Inhib Med. Chem. 37, 451–461.
Dhameja, M., Gupta, P., 2019. Synthetic heterocyclic candidates as promising α-glucosidase inhibitors: an overview. Eur. J. of Med. Chem. 176, 343–377.
Diamant, M., Heine, R.J., 2003. Thiazolidinediones in type 2 diabetes mellitus. Drugs 63, 1373–1406.
Fan, M., Yang, W., Peng, Z., He, Y., Wang, G., 2023. Chromone-based benzohydrazide derivatives as potential α-glucosidase inhibitor: synthesis, biological evaluation and molecular docking study. Bioorg. Chem. 131, 106276.
Fan, M., Yang, W., Liu, L., Peng, Z., He, Y., Wang, G., 2023. Design, synthesis, biological evaluation, and docking study of chromone-based phenylhydrazone and benzoylhydrazone derivatives as antidiabetic agents targeting α-glucosidase. Bioorg. Chem. 132, 106384.
Fan, M., Zhong, X., Huang, Y., Peng, Z., Wang, G.C., 2023. Synthesis, biological evaluation and molecular docking studies of chromone derivatives as potential α-glucosidase inhibitors. J. Mol. Struct. 1274, 134575.
Fettach, S., Thari, F.Z., Hafidi, Z., Karrouchi, K., Bouathmany, K., Cherrah, Y., Achouri, M.E., Benbacer, L., Mzibri, M.E., Sefrioui, H., Bougrin, K., Faouzi, M.E.A., 2023. Biological, toxicological and molecular docking evaluations of isoxazolinethiazolidine-2,4-dione analogues as new class of anti-hyperglycemic agents. J. Biomol. Struct. Dyn. 41, 1072–1084.
Hameed, S., Kanwal, F., Seraj, R., Rafifique, S., Chigurupati, A., Wadood, A.U., Rehman, V., Venugopal, U., Salar, M., Taha, K.M.K., 2019. Synthesis of benzotriazoles derivatives and their dual potential as alpha-amylase and alpha-glucosidase inhibitors in vitro: Structure-activity relationship, molecular docking, and kinetic studies. Eur. J. Med. Chem. 183, 111677.
Heydari, V., Radi, S., Razmjou, A., 2010. Amiri, Chronic complications of diabetes mellitus in newly diagnosed patients. Int. J. Diabetes Mellit. 2, 61–63.
Hu, C.M., Wang, W.J., Ye, Y.N., Kang, Y., Lin, J., Wu, P.P., Li, D.L., Bai, L.P., Xu, X.T., Li, B. Q., Zhang, K., 2021. Novel cinnamic acid magnolol derivatives as potent α-glucosidase and α-amylase inhibitors: Synthesis, in vitro and in silico studies. Bioorg. Chem. 116, 105291.
Huang, J., Zang, X.F., Yang, W.Y., Yin, X.L., Huang, J.P., Wu, S.M., Hong, Y.P., 2021. Pentacyclic triterpene carboxylic acids derivatives integrated piperazine-amino acid complexes for α-glucosidase inhibition in vitro. Bio. Chem. 115, 105212.
Hussain, F., Khan, Z., Jan, M.S., Ahmad, S., Ahmad, A., Rashid, U., Ullah, F., Ayaz, M., Sadiq, A., 2019. Synthesis, in-vitro α-glucosidase inhibition, antioxidant, in-vivo antidiabetic and molecular docking studies of pyrrolidine-2,5-dione and thiazolidine-2,4-dione derivatives. Bioorg. Chem. 91, 103128.
Khan, S., Ullah, H., Rahim, F., Nawaz, M., Hussain, R., Rasheed, L., 2022. Synthesis, in vitro α-amylase, α-glucosidase activities and molecular docking study of new benzimidazole bearing thiazolidinone derivatives. J. Mol. Struct. 1269, 133812.
Lai, D., Li, J., Zhao, S., Gu, G., Gong, X., Proksch, P., Zhou, L., 2021. Chromone and isocoumarin derivatives from the endophytic fungus Xylomelasma sp. Samif07, and their antibacterial and antioxidant activities. Nat. Prod. Res. 35, 4616–4620.
Li, M., Li, L., Lu, L., Xu, X.T., Hu, J., Peng, J.B., 2023. Anti-α-glucosidase, SAR analysis, and mechanism investigation of indolo[1,2-b]isoquinoline derivatives. Molecules 28, 5282.
Li, J., Min, X., Zheng, X., Wang, S., Xu, X., Peng, J., 2023. Synthesis, anti-tyrosinase activity, and spectroscopic inhibition mechanism of cinnamic acid-eugenol esters. Molecules 28, 5969.
Lin, J., Xiao, D., Lu, L., Liang, B., Xiong, Z., Xu, X., 2023. New β-carboline derivatives as potential α-glucosidase inhibitor: Synthesis and biological activity evaluation. J. Mol. Struct. 1283, 135279.
Liu, Y.P., Yu, X.M., Zhang, W., Wang, T., Jiang, B., Tang, H.X., Su, Q.T., Fu, Y.H., 2020. Prenylated chromones and flavonoids from Artocarpus heterophyllus with their potential antiproliferative and anti-inflammatory activities. Bioorg. Chem. 101, 104030.
Lu, L., Zhang, X., Kang, Y., Xiong, Z., Zhang, K., Xu, X., Bai, L., Li, H., 2023. Novel coumarin derivatives as potential tyrosinase inhibitors: synthesis, binding analysis and biological evaluation. Arab. J. Chem. 16, 104724.
Mermer, A., Demirbas, N., Demirbas, A., Colak, N., Ayaz, F.A., Alagumuthu, M., Arumugam, S., 2018. Synthesis, biological activity and structure activity relationship studies of novel conazole analogues via conventional, microwave and ultrasound mediated techniques. Bio. Chem. 81, 55–70.
Özil, M., Parlak, C., Baltas, N., 2017. A simple and efficient synthesis of benzimidazoles containing piperazine or morpholine skeleton at C-6 position as glucosidase inhibitors with antioxidant activity. Bio Chem. 76, 68–77.
Peng, Z., Wang, G., Zeng, Q., Li, Y., Wu, Y., Liu, H., Wang, J., Zhao, Y., 2021. Synthesis, antioxidant and anti-tyrosinase activity of 1,2,4-triazole hydrazones as antibrowning agents. Food Chem. 341, 128265.
Pogaku, V., Gangarapu, K., Basavoju, S., Tatapudi, K.K., Katragadda, S.B., 2019. Design, synthesis, molecular modelling, ADME prediction and anti-hyperglycemic evaluation of new pyrazole-triazolopyrimidine hybrids as potent α-glucosidase inhibitors. Bioorg. Chem. 93, 103307.
Prakash, O., Kumar, R., Parkash, V., 2008. Synthesis and antifungal activity of some new 3- hydroxy-2-(1-phenyl-3-aryl-4-pyrazolyl) chromones. Eur. J. Med. Chem. 43 (2), 435–440.
Saxena, A.R., Gorman, D.N., Esquejo, R.M., Bergman, A., Chidsey, K., Buckeridge, C., Griffiffiffith, D.A., Kim, A.M., 2021. Danuglipron (PF-06882961) in type 2 diabetes: a randomized, placebo-controlled, multiple ascending-dose phase 1 trial. Nat. Med. 27 (6), 1079–1087.
Shaikh, F.M., Patel, N.B., Sanna, G., Busonera, B., La Colla, P., Rajani, D.P., 2015. Synthesis of some new 2-amino-6-thiocyanato benzothiazole derivatives bearing 2, 4-thiazolidinediones and screening of their in vitro antimicrobial, antitubercular and antiviral activities. Med. Chem. Res. 24, 3129–3142.
Shatokhin, S.S., Tuskaev, V.A., Gagieva, S.C., Markova, A.A., Pozdnyakov, D.I., Melnikova, E.K., Bulychev, B.M., Oganesyan, E.T., 2022. Synthesis, cytotoxic and antioxidant activities of new n-substituted 3-(benzimidazol-2-yl)-chromones containing 2,6-di-tert-butylphenol fragment. J. Mol. Struct. 1249, 131683.
Thari, F.Z., Fettach, S., Anouar, E.H., Tachallait, H., Albalwi, H., Ramli, Y., Mague, J.T., Karrouchi, K., Faouzi, M.E.A., Bougrin, K., 2022. Synthesis, crystal structures, α-glucosidase and α-amylase inhibition, DFT and molecular docking investigations of two thiazolidine-2,4-dione derivatives. J. Mol. Struct. 261, 132960.
Wang, G., Peng, Z., Wang, J., Li, X., Li, J., 2017. Synthesis, in vitro evaluation and molecular docking studies of novel triazine-triazole derivatives as potential α-glucosidase inhibitors. Eur. J. Med. Chem. 125, 423–429.
Wang, G., Chen, M., Qiu, J., Xie, Z., Cao, A., 2018. Synthesis, in vitro α-glucosidase inhibitory activity and docking studies of novel chromone-isatin derivatives. Bioorg. Med. Chem. Lett. 28, 113–116.
Wang, G., He, M., Huang, Y., Peng, Z., 2023. Synthesis and biological evaluation of new kojic acid-1,3,4-oxadiazole hybrids as tyrosinase inhibitors and their application in the anti-browning of fresh-cut mushrooms. Food Chem. 409, 135275.
Wu, X., Zhu, W., Lu, L., Hu, C., Zheng, Y., Zhang, X., Lin, J., Wu, J., Xiong, Z., Zhang, K., Xu, X., 2023. Synthesis and anti-α-glucosidase activity evaluation of betulinic acid derivatives. Arab. J. Chem. 16, 104659.
Xiao, D., Lu, L., Liang, B., Xiong, Z., Xu, X., Chen, W.H., 2023. Identification of 1,3,4-oxadiazolyl-containing β-carboline derivatives as novel α-glucosidase inhibitors with antidiabetic activity. Eur. J. Med. Chem. 261, 115795.
Xu, X.T., Deng, X.Y., Chen, J., Liang, Q.M., Zhang, K., Li, D.L., Wu, P.P., Zheng, X., Zhou, R.P., Jiang, Z.Y., Ma, A.J., Chen, W.H., Wang, S.H., 2020. Synthesis and biological evaluation of coumarin derivatives as α-glucosidase inhibitors. Eur. J. Med. Chem. 189, 112013.
Ye, G.J., Lan, T., Huang, Z.X., Cheng, X.N., Cai, C.Y., Ding, S.M., Xie, M.L., Wang, B., 2019. Design and synthesis of novel xanthone-triazole derivatives as potential antidiabetic agents: α-Glucosidase inhibition and glucose uptake promotion. Eur. J. Med. Chem. 177, 362–373.
Zhang, X.L., Li, G.L., Wu, D., Yu, Y.X., Hu, N., Wang, H.L., Li, X.T., Wu, Y.N., 2019. Emerging strategies for the activity assay and inhibitor screening of alpha-glucosidase. Food Funct. 11, 66–82.
Zhang, X., Zheng, Y.Y., Hu, C.M., Wu, X.Z., Lin, J., Xiong, Z., Zhang, K., Xu, X.T., 2022. Synthesis and biological evaluation of coumarin derivatives containing oxime ester as α-glucosidase inhibitors. Arab. J. Chem. 15, 104072.
Zhu, J., Chen, C., Zhang, B., Huang, Q., 2020. The inhibitory effects of flavonoids on alpha-amylase and alpha-glucosidase. Crit. Rev. Food Sci. Nutr. 60, 695–708.